Determination of mechanical properties of the Weld Zone in tailor-welded blanks

J. ROJEK
Institute of Fundamental Technological Research, Polish Academy of Sciences, Pawińskiego 5B, 02-106 Warsaw, Poland

M. HYRCZA-MICHALSKA
Silesian University of Technology, Krasińskiego 8, 40-019 Katowice, Poland

A. BOKOTA, W. PIEKARSKA
Czestochowa University of Technology, Dabrowskiego 69, 42-200 Czestochowa, Poland

Mechanical properties of the weld zone are necessary for accurate modelling of forming processes involving tailor-welded blanks (TWB). Tailored blanks are usually produced by laser welding. Due to small size of the weld cross-section it is not possible to use standard tests to determine mechanical properties of the weld zone in tailor-welded blanks. Special testing procedures must be employed. This paper presents different methods which can be used to determine mechanical properties of the weld zone in tailor-welded blanks. Methods based on experimental tests as well as those combining experimental procedures with numerical studies are described. The presented methods include uniaxial tension tests, microhardness tests and indentation tests combined with inverse numerical analysis. The stress-strain relationships for the weld zone in a steel laser welded blank obtained using different methods have been compared with one another.

Keywords: *tailor welded blanks, mechanical properties, tensile test, indentation, inverse analysis*

1. Introduction

Various benefits, like part integration, tooling cost reduction, weight reduction and improvement of structural properties, have extended the use of tailor welded blanks (TWB) in the car design and manufacturing. Tailor welded blanks are produced by welding together blanks (or sheets of metal) of different grades or thicknesses. Despite a widespread use the design and stamping of the parts from TWBs still present certain difficulties. Forming properties of TWBs are considerably different from those of homogenous blanks. Main factors influencing the formability of TWBs are the difference in material properties and/or thickness of the welded blanks, change of the material properties in the weld and heat-affected zones (HAZ) as well as location and orientation of the weld line [4,14]. In steel TWBs, in general, the weld is characterized with higher strength and lower ductility than base materials [12]. Therefore the formability in the area of the weld is significantly reduced. On the contrary to steel TWBs, the weldment in an aluminum TWB is usually the weakest region so the

formability of the TWB critically depends on the mechanical properties of the weldment [9,18].

The properties and forming behavior of TWBs have been widely studied experimentally [2,12]. Experimental investigations of TWBs are often combined with numerical studies [5,11,12]. Numerical simulation enables a better understanding of the forming behaviour and failure mechanisms during forming of TWBs.

Finite element analysis of forming of TWB is performed by two methods, i.e., either by considering the weld region as a weld line along which the blanks are tied together [12,19] or as separate weld zone with specified material properties distinct from those of the base materials [11,15]. Heat affected zones can also be included in TWB models as separate entities in addition to the weld zone and base materials [14]. Various finite element models for TWB, employing discretization with solid and shell elements, both with and without weld zone, are compared in terms of accuracy and cost effectiveness by [19]. Inclusion of the weld zone, however, improves the analysis results, especially if failure occurs near the weld region [11]. The importance of treating the weld region, either as a zone or as a line, in FE simulations has been investigated by [10].

Accurate modelling of tailor welded blanks with the weld included as a separate weld zone requires knowledge of mechanical properties of material in the weld zone as well as its geometry (width, area). Determination of mechanical characteristics of the weld zone in TWB is not an easy task because of small extension of this zone. Different methods are available to determine mechanical properties of the weld zone.

In order to determine the stress-strain relationship of the weld bead, Saunders [17] developed an analytical procedure based on separation of the load supported by the base material from that supported by the weld. The procedure was applied to the results of tensile tests performed with specimens cut from base material and from welded blank in such a way that the weld was along the loading direction. Similar methodology to extract mechanical properties of the weld zone in TWBs was employed by [1]. In this case, however, the authors used specimens of different size claiming the smaller specimens allowed them to obtain more accurate results. Tensile properties of the material in the weld zone of TWBs were measured directly using a specially designed specimens for weldments by [3]. Mechanical properties of the weld zone in TWBs can also be assessed indirectly with the help of micro-hardness measurements [14,16].

Most of the cited above works concentrate on one method. The purpose of this article is to review and critically assess different available methods to determine data necessary to model the weld zone of TWBs. The extension of the weld zone will be studied by metallographic observations and microhardness tests. The tensile properties of the material in the weld zone will be determined by the tensile tests using specimens without weld and with weld parallel to the loading direction. Alternatively tensile properties will be determined indirectly using the results of microhardness measurements as well as indentation tests combined with inverse analysis based on the

finite element simulation of these tests. Additionally mechanical properties will be determined numerically by simulating the laser welding process. The results obtained using different methods will be compared in terms of accuracy and practical use. Validity of assumptions made for different testing procedures is explored.

2. Metallographic observations

In this study, tailor welded blanks were obtained by joining steel sheets (1000 mm × 150 mm) of the grade DC04 and of the thickness 1.0 mm. In order to avoid the effect of difference in thickness and properties of base materials on the weld characteristics, the two identical base sheets are taken for the investigations presented in this paper. The TWBs were welded using a Nd:YAG laser.

Mechanical properties of the weld are related to the microstructure after welding which can be investigated by metallographic observations. Observations of microstructure of the weld zone of a TWB provide information about the extension of the fusion and heat-affected zones, as well as phase composition in these zones. Microstructure of steel was investigated with the use of optical and transmission electron microscopes. The primary microstructure of steel before welding consisted of ferrite with a little contribution of pearlite (about 8%). It was found that after welding the microstructure of TWB specimen (in the weld and heat affected zone) is composed of about 50% of bainite, 45% of ferrite and 5% of martensite (Fig. 1). The results of metallographic observations will be used as reference data for validation of welding simulation.

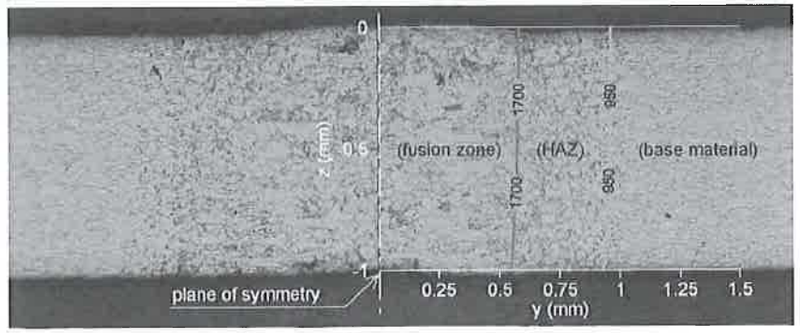

Figure 1. Microstructure of the investigated TWB

3. Uniaxial tension tests

Uniaxial tension test yielding a stress–strain curve is one of the basic tests to determine mechanical properties of a material. Standard tensile tests can be applied to the base material of a TWB, testing of the material of the weld zone, however, requires some modification. Due to small size of the weld cross-section it is not

possible to use standard size specimens. Following the procedure presented in [1] specimens of different size have been used for testing. Some specimens have been cut out from the base material only, and the others have been cut from the material with the weld in such a way the weld line was parallel to the loading direction and coincided with the axis of symmetry of the specimens.

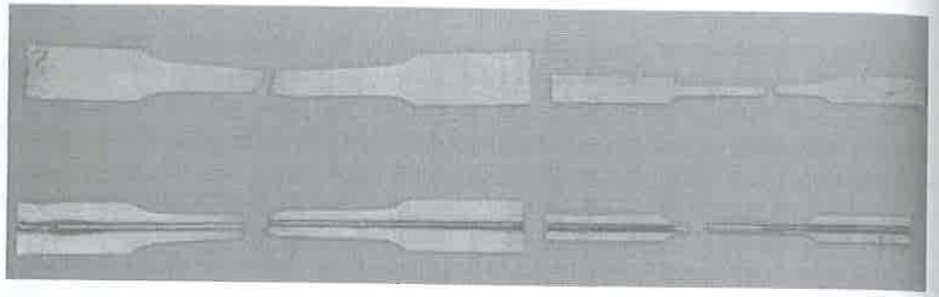

Figure 2. Broken specimens after tensile testing

Broken specimens after tensile tests are shown in Fig. 2. Representative stress–strain curves obtained for different specimens are plotted in Fig. 3 using engineering stress and strain measures. The curves obtained for the specimens without weld characterize strength properties of the parent (base) material. The agreement between the curves obtained with different sizes can be observed, this means that the small specimens are adequate for tensile testing. It can be seen that the strength of the specimens with weld is higher than that of the specimens without weld. The influence of the weld material strengthening can be clearly observed. The weld also decreases the maximum elongation of the tested material. The effect of the weld in the small specimen is more pronounced.

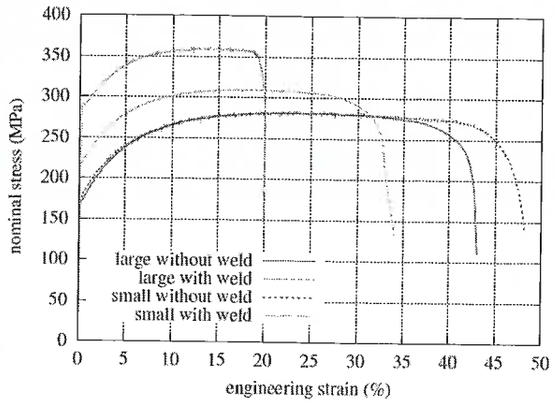

Figure 3. Engineering stress-strain curves for different specimens

Numerical analysis of TWB forming requires the input of stress–strain curves in true stress and true strain measures. Under assumption of uniform deformation the true (Cauchy) stress σ_t and true (logarithmic) strain ε_t can be expressed in terms of engineering (nominal) stress σ_e and engineering strain ε_e

$$\sigma_t = \sigma_e(1+\varepsilon_e) \tag{1}$$

$$\varepsilon_t = \ln(1+\varepsilon_e) \tag{2}$$

Using equations (1) and (2) in the range of the deformation up to the initiation of necking true stress–true strain curves can be obtained from engineering stress-strain curves. The curves computed by this procedure for different specimens are plotted in Fig. 4.

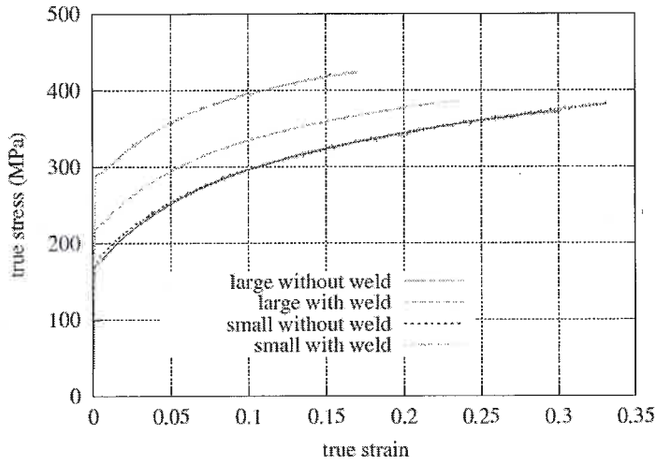

Figure 4. True stress-true strain curves obtained for different specimens

The stress–strain curve for the material in the weld zone can be extracted from the curves characterizing tensile properties of the weld with and without weld. The resultant force, P, in the specimen with weld can be written in terms of average stresses, σ_t^{spw}, as

$$P = \sigma_t^{spw} A^{spw} \tag{3}$$

where A^{spw} is the cross-sectional area of the specimen with weld. The load P can be decomposed into the parts carried by the weld and base material, P^w and P^{bm}, respectively:

$$P = P^w + P^{bm} = \sigma_t^w A^w + \sigma_t^{bm} A^{bm} \tag{4}$$

where σ_t^w and σ_t^{bm} are average stresses in the weld and in the base material, respectively, in the loaded specimen with weld, A^w is cross-sectional area of the weld and A^{bm} is the cross-sectional area corresponding to the base material, the following equality being satisfied

$$A^{spw} = A^w + A^{bm} \tag{5}$$

Combining Eqs. (3) and (4) the expression for the stresses in the weld can be obtained in the following form:

$$\sigma_t^w = \sigma_t^{spw} \frac{A^{spw}}{A^w} - \sigma_t^{bm} \frac{A^{bm}}{A^w} \tag{6}$$

Assuming that the weld and base material in the specimen deform uniformly, the ratios A^{spw}/A^w and A^{bm}/A^w are constant during the deformation until the initiation of the failure and can be estimated from the metallographic observations of the TWB cross-section. Estimating the average width of weld zone (including the fusion zone and heat affected zones) in the TWB investigated to be 2.1 mm (Fig. 1) and applying the procedure expressed by Eq. (6) to small and large specimens with weld the stress–strain curves for the material in the weld are obtained. The curves are plotted in Fig. 5 in comparison with the curves for the base material. A very good agreement can be

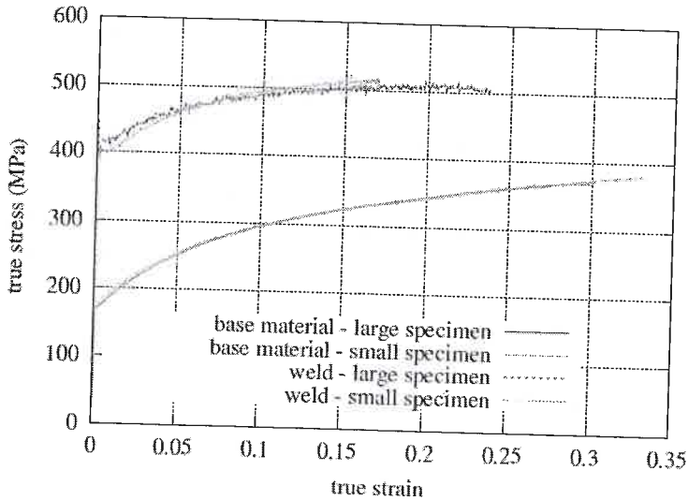

Figure 5. True stress-true strain curves for base material and weld

observed between the curves obtained for the specimens of different size. The stress–strain curves obtained from the tension tests are treated as the reference one for curves produced by other methods.

Many computer programs for simulation of forming processes require the curves given analytically. One of the most common analytical approximations of the stress-strain curves is that given by the Swift equation [6]:

$$\sigma = C(\varepsilon_0 + \varepsilon_{eff}^p)^n \tag{7}$$

where C, ε_0 and n are the material parameters and ε_{eff}^p is the effective plastic strain. The Swift approximation of the curves for the weld and base materials are shown in Fig. 6. The Swift parameters for the base material are the following: $C = 491$ MPa, $\varepsilon_0 = 8.119 \cdot 10^{-3}$ and $n = 0.22579$. The analytical curve for the weld is defined by the following Swift model parameters: $C = 603.8$ MPa, $\varepsilon_0 = 4.069 \cdot 10^{-3}$ and $n = 8.897 \cdot 10^{-2}$.

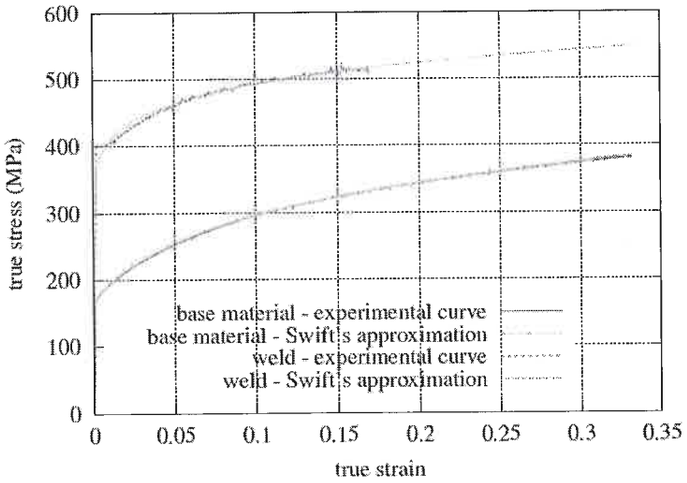

Figure 6. Experimental true stress-true strain curves for base material and weld and their analytical approximations

4. Microhardness test

Microhardness tests provide information about the distribution of hardness in the tailor weld blank. This indicates the extension of the weld zone. Having obtained the hardness, the relationship between hardness and strength of the material allows us to determine strength parameters of the weld zone.

Microhardness measurements have been made for the tailor welded blank under investigation using a Vicker's microhardness tester. The scale HV 0,2 with the loading

of 1.961 N has been employed. Microhardness has been measured on the blank surface along the line perpendicular to the weld.

The results of microhardness measurements are plotted in Fig. 7. It can be observed that material in the weld zone is characterized with much higher hardness (approximately 1800 MPa) than the base material (approximately 1050 MPa). The weld zone extension determined by the microhardness measurements (Fig. 7) coincides with the extension estimated in metallographic observations (Fig. 1).

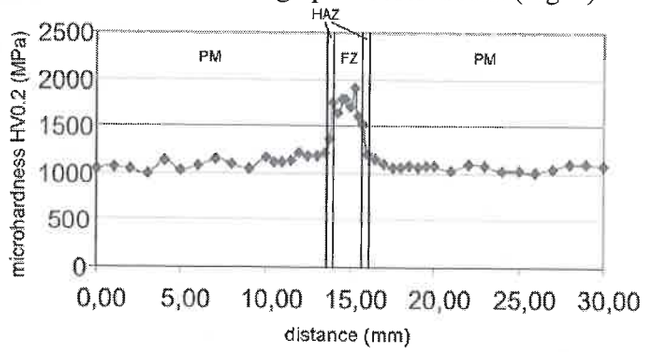

Figure 7. Microhardness profile along the line perpendicular to the weld

Experimental investigations show that both the yield strength and tensile strength of steels exhibit a linear correlation with the hardness [13]. Assuming that the strength is represented by the yield stress, we can write the following relationship between the yield stress and hardness of the weld and base material, σ^{w} and μH^{w}, and σ^{bm} and μH^{bm}:

$$\frac{\sigma^{w}}{\mu H^{w}} = \frac{\sigma^{bm}}{\mu H^{bm}} \tag{8}$$

This means that knowing the stress-strain curve of the base material the stress-strain curve of the weld material can be obtained as

$$\sigma^{w} = \sigma^{bm} \frac{\mu H^{w}}{\mu H^{bm}} \tag{9}$$

The stress-strain curve for the weld obtained by scaling the curve of the base material is given in Fig. 8. Comparison with the curve obtained from the tension tests (Fig. 8) shows that scaling (9) underestimates the yield stress in the range of small plastic deformation and overestimates the yield stress in the range of large plastic deformation.

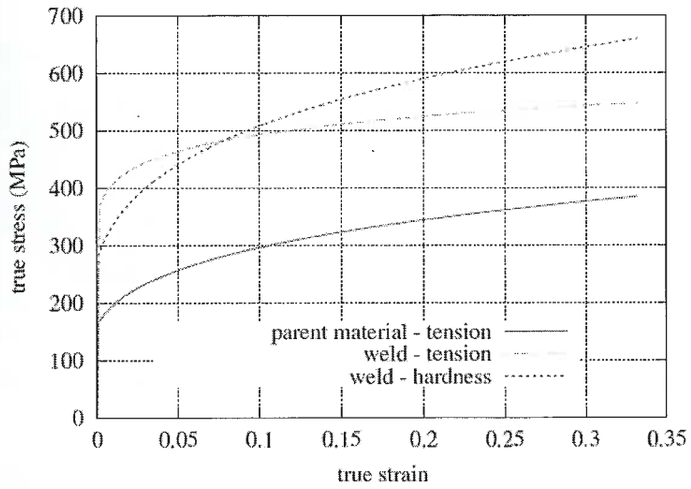

Figure 8. Stress-strain curves for weld and base material obtained from the microhardness measurements

5. Indentation tests

Indentation tests basically involve the same testing procedure as that used in hardness measurements but unlike in the latter tests the former methods employ the results to extract more information about the material behaviour. The load-unload curve obtained during indentation is commonly used to identify mechanical properties of the material [7, 8].

Indentation tests have been made on the studied tailor welded blank. The test points have been chosen in different places of both base material and weld zone. The results of these tests combined with an inverse numerical analysis have allowed us to determine mechanical properties of both base material and weld zone. Indentation tests have been performed using a Rockwell hardness tester and assuming the hardness scale HR15T with a steel ball indentor 1/16″. Typical results of the indentation tests are shown in Figs. 9 and 10.

Material properties have been determined by fitting simulation and experimental force vs. indentation depth curves. As the target experimental curves we take the curves shown in Fig. 9a and 10a for the base material and for weld material, respectively. The inverse problem can be defined as an optimization problem. In our case we used a simple trial-and-error approach. Numerical results of simulation of indentation tests for the weld material are shown in Figs. 11 and 12 in the form of the deformed configuration with distribution of equivalent plastic strain and the numerical curve force vs. depth of indentation, respectively. Similar results are obtained for the weld zone (Fig. 13).

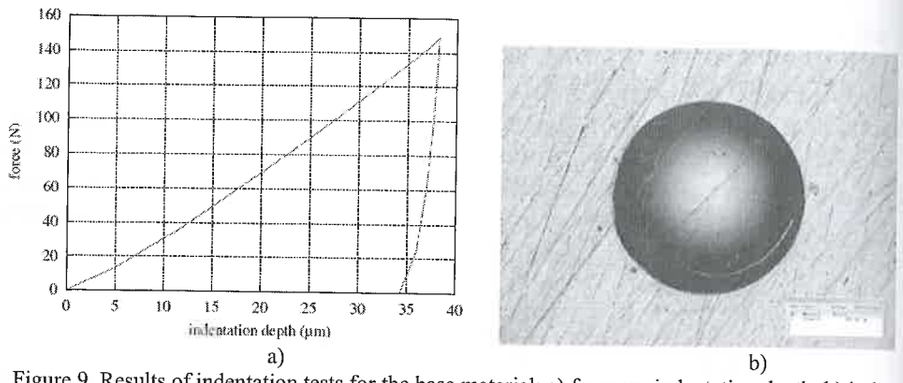

a) b)

Figure 9. Results of indentation tests for the base material: a) force vs. indentation depth, b) indentation diameter 494.88 μm

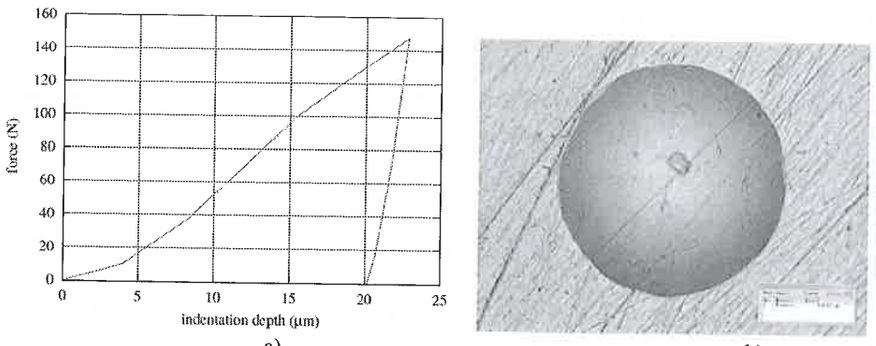

a) b)

Figure 10. Results of indentation tests for the weld zone: a) force vs. indentation depth, b) indentation diameter 341.43 μm

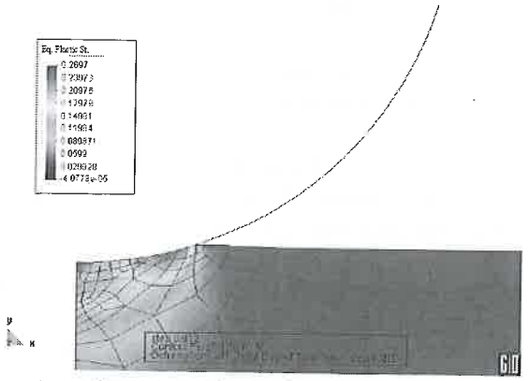

Figure 11. Numerical results of simulation of indentation tests for the base material – evolution of deformed configuration with distribution of equivalent plastic strain

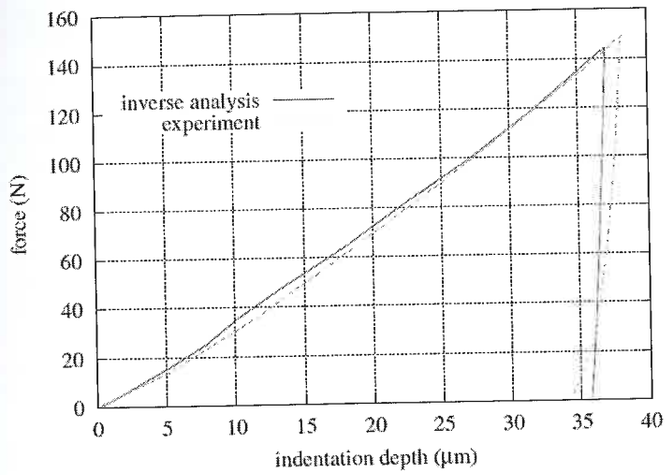

Figure 12. Fitting of numerical vs. experimental force-indentation depth curves for the base material

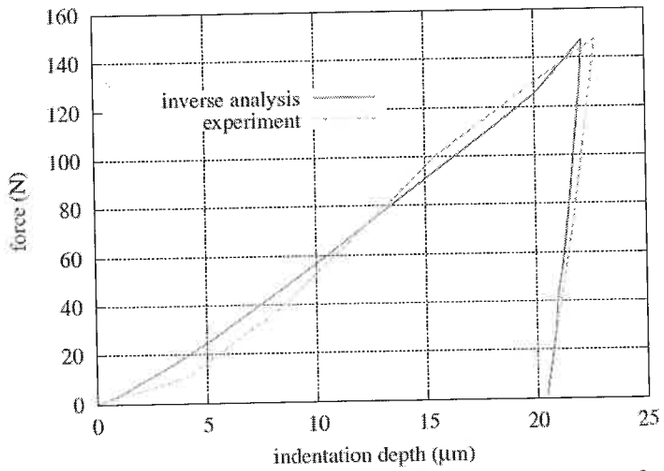

Figure 13. Fitting of numerical vs. experimental force-indentation depth curves for the weld zone

Stress-strain curves for the weld and base material obtained from the inverse analysis are shown in Fig. 14 in comparison with the reference curves obtained from the tension tests. The curve for the base material obtained from indentation tests gives slightly lower stresses than those determined by the tension tests, hardening parameters of both curves, however, are similar. Comparison of the curves for the weld material indicates that the initial yield stress predicted by the indentation tests is lower than that obtained from the tension tests, and hardening from the indentation tests is higher than that obtained from the tension tests.

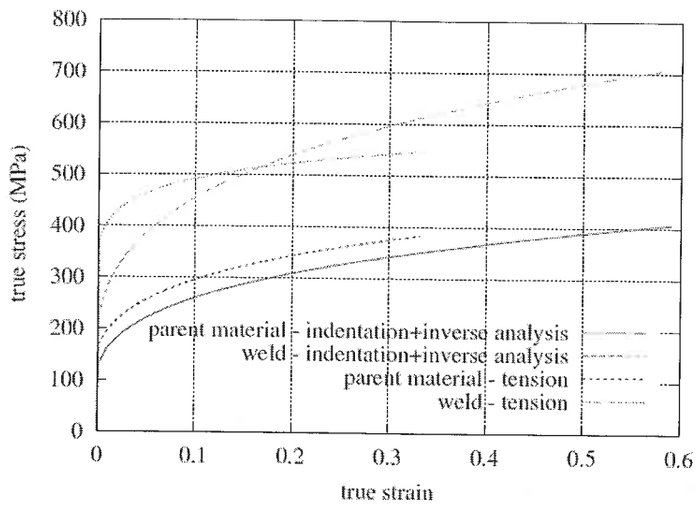

Figure 14. Stress-strain curves for weld and base material obtained from the inverse analysis

6. Conclusions

Different methods, including metallographic observations, uniaxial tension tests, microhardness measurements, indentation tests and numerical simulation of laser welding, are available for determination of mechanical and geometrical characteristics of the weld zone in tailor welded blanks. The stress–strain curves obtained. with different methods show certain differences although the level of stresses is similar. The tensile test can be considered as the most trustworthy method to determine stress–strain curve as the curve is a direct result of the test. The methodology consisting in using the specimens with weld along the loading direction gives a stress-strain curve for a material in a weld. Comparison of the results obtained using standard and small specimens indicates that both sizes give similar results as the yield stress and hardening of the material in a weld zone are concerned, therefore standard specimens can be used for testing.

References

[1] Abdullah K., Wild P.M., Jeswiet J.J., Ghasempoor A.: *Tensile testing for weld deformation properties in similar gage tailor welded blanks using the rule of mixtures*, Journal of Materials Processing Technology, Vol. 112, 2001, pp. 91–97.

[2] Chan S.M., Chan L.C., Lee T.C.: *Tailor-welded blanks of different thickness ratios effects on forming limit diagrams*, Journal of Materials Processing Technology, Vol. 132, 2003, pp. 95–101.

[3] Cheng C.H., Chan L.C., Chow C.L.: *Weldment properties evaluation and formability study of tailor-welded blanks of different thickness combinations and welding orientations*, J. Mater. Sci., Vol. 42, 2007, pp. 5982–5990.

[4] Hyrcza-Michalska M., Rojek J., Fruitos O.: *Numerical simulation of car body elements pressing applying tailor welded blanks – practical verification of results*, Archives of Civil and Mechanical Engineering, Vol. X, 2010, No. 4, pp. 31–44.

[5] Jie M., Cheng C.H., Chan L.C., Chow C.L., Tang C.Y.: *Experimental and Theoretical Analysis on Formability of Aluminum Tailor-Welded Blanks*, Journal of Engineering Materials and Technology, Vol. 129, 2007, pp. 151–158.

[6] Kleemola H.J., Nieminen M.A.: *On the strain-hardening parameters of metals*, Metallurgical Transactions B, Vol. 5, 1974, pp. 1863–1866.

[7] Kucharski S., Mróz Z.: *Identification of plastic hardening parameters of metals from spherical indentation tests*, Materials Science & Engineering, Vol. 318, 2001, pp. 65–76.

[8] Kucharski S., Mróz Z.: *Identification of hardening parameters of metals from spherical indentation test*, Journal of Engineering Materials and Technology – Trans. ASME, Vol. 123, 2004, pp. 245–250.

[9] Miles M.P., Decker B.J., Nelson T.W.: *Formability and Strength of Friction-Stir-Welded Aluminum Sheets*, Metallurgical and Materials Transactions A, Vol. 35, 2004, pp. 3462–3468.

[10] Narayanan R.G., Narasimhan K.: *Weld Region Representation during the Simulation of TWB Forming Behavior*, International Journal of Forming Processes, Vol. 9, No. 4, 2006, pp. 491–518.

[11] Narayanan R.G., Narasimhan K.: Predicting the forming limit strains of tailor-welded blanks, J. Strain Analysis, Vol. 43, 2008, pp. 551–563.

[12] Panda S.K., Kumar D.R., Kumar H., Nath A.K.: *Characterization of tensile properties of tailor welded if steel sheets and their formability in stretch forming*, Journal of Materials Processing Technology, Vol. 183, 2007, pp. 321–332.

[13] Pavlina E.J., Van Tyne C.J.: *Correlation of yield strength and tensile strength with hardness for steels*, Journal of Materials Engineering and Performance, Vol. 17, 2008, pp. 808–893.

[14] Piela A., Rojek J.: *Validation of the results of numerical simulation of deep drawing of tailor welded blanks*, Archives of Metallurgy, Vol. 48, 2003, pp. 37–51.

[15] Qiu X.G., Chen W.L.: *The study on numerical simulation of the laser tailor welded blanks stamping*, Journal of Materials Processing Technology, Vol. 187-188, 2007, pp. 128–131.

[16] Reis A., Teixeira P., Ferreira Duarte J., Santos A., Barata da Rocha A., Fernandes A.A.: *Tailored welded blanks – an experimental and numerical study in sheet metal forming on the effect of welding*, Comput. Struct., Vol. 82, 2004, pp. 1435–1442.

[17] Saunders F.I.: *Forming of tailor-welded blanks*, PhD thesis, Ohio State University, Columbus, 1994.

[18] Wu N.Q., Xia C., Li M., Perrusquia N., Mao S.X.: *Interfacial Structure and Micro and Nano-Mechanical Behavior of Laser-Welded 6061 Aluminum Alloy Blank*, Journal of Engineering Materials and Technology, Vol. 126:8–13, 2004.

[19] Zhao K.M., Chun B.K., Lee J.K.: *Finite element analysis of tailor-welded blanks*, Finite Elements in Analysis and Design, Vol. 37, pp. 117–130, 2001.